

Loredo, C., Ordóñez, A., Garcia-Ordiales, E., Álvarez, R., Roqueñi, N., Cienfuegos, P., Peña, A., and Burnside, N.M. (2017) Hydrochemical characterization of a mine water geothermal energy resource in NW Spain. *Science of the Total Environment*, 576, pp. 59-69.(doi:[10.1016/j.scitotenv.2016.10.084](https://doi.org/10.1016/j.scitotenv.2016.10.084))

This is the author's final accepted version.

There may be differences between this version and the published version. You are advised to consult the publisher's version if you wish to cite from it.

<http://eprints.gla.ac.uk/133059/>

Deposited on: 20 December 2016

## Hydrochemical characterization of a mine water geothermal energy resource in NW Spain

C. Loreda<sup>a</sup>\*, A. Ordóñez<sup>a</sup>, E. Garcia-Ordiales<sup>a</sup>, R. Álvarez<sup>a</sup>, N. Roqueñi<sup>a</sup>, P. Cienfuegos<sup>a</sup>, A. Peña<sup>b</sup>, N.M. Burnside<sup>c</sup>.

<sup>a</sup>Dep. Explotación y Prospección de Minas. University of Oviedo, Spain. Independencia, 13. 33004 Oviedo, Asturias \*corresponding author ([loredocovadonga@uniovi.es](mailto:loredocovadonga@uniovi.es))

<sup>b</sup>Hulleras del Norte, S. A. (HUNOSA), Avenida de Galicia 44, ES-33005 Oviedo, Spain

<sup>c</sup>School of Engineering, University of Glasgow, G12 8QQ, UK

### ABSTRACT

Abandoned and flooded mine networks provide underground reservoirs of mine water that can be used as a renewable geothermal energy source. A complete hydrochemical characterization of mine water is required to optimally design the geothermal installation, understand the hydraulic behaviour of the water in the reservoir and prevent undesired effects such as pipe clogging via mineral precipitation. Water pumped from the Barredo-Figaredo mining reservoir (Asturias, NW Spain), which is currently exploited for geothermal use, has been studied and compared to water from a separate, nearby mountain mine and a river that receives mine water discharge and partially infiltrates into the mine workings. Although the hydrochemistry was altered during the flooding process, the deep mine waters are currently near neutral, net alkaline, high metal waters of Na-HCO<sub>3</sub> type. Isotopic values suggest that mine waters are closely related to modern meteoric water, and likely correspond to rapid infiltration. Suspended and dissolved solids, and particularly iron content, of mine water results in some scaling and partial clogging of heat exchangers, but water temperature is stable (22°C) and increases with depth, so, considering the available flow (>100 L s<sup>-1</sup>), the Barredo-Figaredo mining reservoir represents a sustainable, long-term resource for geothermal use.

**Keywords:** geothermal energy; mine water; hydrochemistry; isotopic study; clogging

### 1. INTRODUCTION

Flooded mine workings host groundwater reservoirs that can be exploited for geothermal energy generation. The thermal resource potential of mine water is widely recognised, and a number of geothermal investigations at former mining sites (particularly coal mines) have either been completed, or are underway (Burnside et al., 2016a and b; Peralta et al., 2015; Preene and Younger, 2014; Hall et al., 2011; Hamm and Bazargan, 2010; Raymond and Therrien, 2007; Watzlaf and Ackman, 2006, among others).

Underground mine workings can reach hundreds of meters of depth and the network of shafts and galleries within the workings provides an enormous heat exchange interface with exposed, comparatively warm, rock faces (Banks, 2016). The temperature of post-abandonment flood waters is shielded from seasonal atmospheric temperature variations and so is ca. stable and maintained at advantageously high enough values to be utilised for heating purposes through the use of heat pumps. However, geothermal use of mine water is complex and requires thorough investigation in order to make best use of and effectively manage the thermal resource. A detailed hydrogeological characterization of the mining reservoir is a necessity if one is to fully appreciate subsurface hydrological behaviour and determine the long-term suitability of flooded mines as a sustainable thermal resource. This can be particularly difficult in old, long abandoned, flooded mines due to the lack of knowledge about the location and condition of underground mine workings. In many cases, the volume of voids can be estimated and the flooding process can be monitored, allowing for parallel development of hydraulic reservoir models of the reservoir and an intimate understanding of recharge rates and sources (i.e. available water resources) which are essential for optimal geothermal exploitation (Ordóñez et al., 2012; Jardón et al., 2013). The long-term temperature of the mine water reservoir, particularly under

different scenarios of water extraction, use and injection is of key concern and several models have been implemented to predict it (Loredo et al., 2016; Andrés et al., 2015; Uhlík and Baier, 2012; Raymond et al., 2011; Blöcher et al., 2010; Renz et al., 2009).

The study of physiochemical, major ion and isotope values allows for interpretation of origin and age of infiltrated waters (Ozyurt et al., 2014) and helps to constrain the hydrological behaviour of the system (i.e. water inputs from different galleries, connections between shafts, flooding effects, mixing with deep saline waters, etc.). In addition, water quality variations can be related to depth and to effects of the exploitation method (mixing induced by pumping, effect of reinjection, pumping at different depths, etc.). Detailed hydrogeochemical studies of pumped mine waters in the UK (Burnside et al. 2016a and b) and Poland (Janson et al. 2016) have revealed much about the history and subsurface mixing of mine waters, provided vital information for geothermal projects, and have laid the foundations for further mine water geothermal investigations, such as this one.

The chemical composition of mine water (i.e. hardness, iron content, etc.) can limit its application, as certain waters are prone to precipitation on pipes or heat exchangers, leading to scaling or so-called clogging or fouling (Garrido et al., 2016). The accretion of deposits decreases thermal transfer, increases flow resistance, and ultimately reduce the system's performance. Ideally, water pH should be maintained between 6 - 8.5, the concentrations of calcium, chlorides, dissolved solids, iron and nitrates should be below 800, 5, 500, 3 and 10 mg·L<sup>-1</sup>, respectively, and levels of dissolved carbon dioxide and oxygen should be kept to a minimum (MTS Systems Corporation, 2005; Butterworth, 2002). The main objective of this study is to characterize the chemistry and isotopic composition of the mine water used in the Barredo-Figaredo system (Mieres, Asturias, NW Spain) in order to determine features that could affect the short and long-term performance and sustainability of the existing installation and, in addition, identify key parameters to define future monitoring strategies at other mine water projects.

## 2. STUDY AREA

This study focusses on Barredo-Figaredo mine water reservoir, located in the Asturian Central Coal Basin (CCB; NW Spain), close to the city of Mieres (Fig. 1). Historically in the CCB, a first phase of "mountain mining" was undertaken from the level of the valleys to the highest outcrop of the coal layers. Once it was depleted, exploitation continued through vertical or inclined shafts to access lower levels (deep or "underground mining"). The Barredo underground mine was active from 1926 to 1993. It has 5 levels and a total depth of 360 m. The extractive activity of the Figaredo mine lasted from the second half of the 19th century to 2007, reaching a maximum depth of 650 m. Both mines are clearly connected through faces and galleries at -135, -29 and +23 m.a.s.l. and they constitute a hydrogeologically isolated system (Fig. 2); Figaredo workings are supposed to be interconnected with other neighbouring mines, such as San Jose and Santa Barbara, but these connections were proven to be ineffective during the inundation period (Ordóñez et al., 2012). When active mining was taking place, an average water volume of 4 million m<sup>3</sup> per year was pumped from this system. In 2008 pumping ceased and about one year later the mining voids were flooded up to a depth of 70 m below the surface at the Barredo site, suggesting addition of up to 5.8 million m<sup>3</sup> of water. Besides recharge from effective rainfall infiltration, the reservoir receives recharge from the Turón River, which loses part of its flow as it crosses the most mined and fractured zones of the Figaredo mine workings (Ordóñez et al., 2012). The water recharging the reservoir has to be permanently pumped to maintain a safe flood level; a small portion of this pumped water is used but it is mostly discharged to the local watercourse. Upstream, the Turón River receives inflow from the San José and Santa Bárbara mines, which are interconnected (but isolated in the subsurface from Barredo-Figaredo) (Fig. 1). These mines reached a depth up to 550 m b.g.l, and have flooded since their closure in 1994. Pumping is maintained at San José shaft, with an average flow of 115 L·s<sup>-1</sup>, and discharged into Turón River. In addition, around 100 m from the Barredo shaft there is a mountain mine, called

Mariana, which was previously connected with Barredo but this connection is currently sealed. All of these mines are maintained by the mining company HUNOSA.

The geology of the CCB consists of very thick (up to 6000 m) sedimentary sequences of Westphalian (Mid-Pennsylvanian) age. Quantitatively, marine facies are more important than continental or transitional rocks. Main lithofacies include mudstones, siltstones, sandstones (litharenites), coal seams and minor quantities of limestones and conglomerates. Westphalian rocks are divided, from bottom to top into two major units, known as Lena and Sama Groups. Coal seams are located in the upper part (Westphalian-D in age) of the stratigraphic column (for more detail see García-Loygorri et al. (1971) and Piedad-Sánchez et al. (2004)). The area of study is constituted by the youngest sub-unit of Lena Group (Caleras mining pack) and the oldest sub-units of the Sama Group (Generalas, San Antonio, María Luisa, Sotón and Entrerregueras mining packs; Fig. 2). The whole terrigenous-dominated synorogenic succession was highly deformed during the Hercynian cycle, being affected by kilometric-scale superposed folding (Aller and Gallastegui, 1995), with a first generation of N-S trending folds superposed by secondary E-W trending folds. These late structures are thought to have been reactivated during the N-S Alpine compression (Alonso et al., 1996). The stratigraphy is generally of a low permeability, except for some minor, higher permeability terrestrial units. The voids generated by several decades of coal extraction, and fracturing associated with orogenic events, have created the current underground reservoir, with hydrogeological behaviour similar to a karst aquifer (Ordóñez et al. 2012).

Mine water is currently pumped from the Barredo shaft at a depth of 100–200 m below the land surface at a temperature  $>20^{\circ}\text{C}$ . According to the thermal profiles measured by HUNOSA inside this shaft, the 4 upper sections display seasonal temperature variations, whereas the temperature is more stable in the lower part of the mine. Stratification breakdown due pumping allows for mixing of waters of different temperatures and can potentially lead to negative effects on the thermal resource (Andrés et al., 2015; Wolkersdorfer, 2008). Water stored in Barredo-Figaredo reservoir is currently used as a geothermal resource to supply heating and cooling to several public buildings i.e. University, FAEN (Regional energy agency) and the new Álvarez-Buylla Hospital. Two heat pumps of 352 kW have been installed at the University building, two 1.2 MW and a 652 kW heat pumps supply heat to the Hospital and a 100 kW heat pump has recently been put into operation at FAEN. Water temperatures reported from other mine water projects range between  $12^{\circ}\text{C}$  (Shettleston, Scotland) and  $21^{\circ}\text{C}$  (Nowa Rudat, Poland), being the majority of values between  $14$  and  $18^{\circ}\text{C}$  ( $14^{\circ}\text{C}$  for Park Hills –USA- and Lumphinnans –UK- mines,  $16$ – $18^{\circ}\text{C}$  for Heerlen –Netherlands- and  $18^{\circ}\text{C}$  for Spring Hills mine –Canada) (Hall et al. 2011). Taking this account, the Barredo-Figaredo reservoir constitutes an attractive geothermal resource. A technical and economic analysis of the potential of the mine water from this reservoir is detailed in Jardón et al. (2013); the long term sustainability of the system in terms of temperature inside the reservoir was proven in Andrés et al. (2015). Increasing geothermal use gave rise to the need to better characterize the mine water from Barredo and Figaredo mines so as to better understand the optimal use and long-term sustainability of the thermal resource. The work presented in this paper represents the initial hydrochemical investigation of mine waters pumped from Barredo and Figaredo shafts and compares them to waters from the Mariana mountain mine and the Turón River.

### 3. METHODS

This work focusses on the analysis of water from different interrelated environments (mine water, river water and rainfall), as well as the precipitates originated from mine water. Seven sampling campaigns (from January 2015 to February 2016, every 2–3 months) were undertaken, taking water from Barredo and Figaredo mines, Mariana mine drainage and the Turón River (8 sampling points). There are two pumps in the Barredo shaft (at 100 and 200 m b.g.l.), so samples were taken when each individual pump was in operation, and when both were pumping simultaneously. The pump at Figaredo shaft is 100 m deep. Samples in the river were taken both upstream of all the mines in the basin and downstream of San José mine (Fig. 1). Samples of mine water

from Barredo, before and after passing through the plate heat exchanger of the geothermal installation, were also taken. In addition, rainfall was sampled to determine its isotopic signature.

Field measurements of temperature, pH, oxidation-reduction potential (Eh), electrical conductivity and total dissolved solids (TDS) were undertaken by means of a HANNA HI 9829 multiprobe. Alkalinity was also measured in situ by titration using a Merck phenolphthalein Alkalinity test. Major ions ( $\text{Ca}^{2+}$ ,  $\text{Mg}^{2+}$ ,  $\text{Na}^+$ ,  $\text{K}^+$ ,  $\text{HCO}_3^-$ ,  $\text{SO}_4^{2-}$ ,  $\text{Cl}^-$ ,  $\text{NO}_3^-$ ) and some minor ions ( $\text{Li}^+$ ,  $\text{NH}_4^+$ ,  $\text{F}^-$ ,  $\text{Br}^-$ ,  $\text{NO}_2^-$ ,  $\text{PO}_4^{3-}$ ) were analysed by ionic chromatography (METROHM 883 IC plus). Dissolved Fe and Mn were analysed using an Atomic Absorption Spectroscopy (AAS) method in samples filtered through 0.45  $\mu\text{m}$  Teflon filters to exclude suspended particulate matter and preserved with  $\text{HNO}_3$  (1% v/v) to  $\text{pH} < 2$  to prevent any precipitation. Additional samples were acidified, but not filtered, to determine total Fe and Mn concentrations. Total Carbon (TC) and Dissolved Inorganic Carbon (IC) were determined by means of a Shimadzu TOC-V CSH instrument. Dissolved Organic Carbon (DOC) was obtained by difference. All laboratory analysis was completed at the facilities of the University of Oviedo. Ionic species in water solution as well as the 5 saturation indexes for mineral phases were obtained using the software PHREEQC (Parkhurst and Appelo, 1999).

Stable isotope analyses were undertaken at the Scottish Universities Environmental Research Centre (SUERC) laboratories, East Kilbride, and full details of procedure can be found in Burnside et al. (2016). Samples of water for  $\delta^{18}\text{O}$  and  $\delta^2\text{H}$  were taken in triplicate using clean 10 ml screwcap glass vials sealed with Parafilm to prevent any evaporation.  $\delta^{18}\text{O}$  analysis was carried out on a Thermo Scientific Delta V mass spectrometer and final  $\delta^{18}\text{O}$  values were produced using the method established by Nelson (2000).  $\delta^2\text{H}$  values were determined using a VG Optima mass spectrometer. Final values for  $\delta^{18}\text{O}$  and  $\delta^2\text{H}$  are reported as per mil (‰) variations from the V-SMOW standard in standard delta notation. In-run repeat analyses of water standards (international standards V-SMOW and GISP, and internal standard Lt Std) gave a reproducibility better than  $\pm 0.3\text{‰}$  for  $\delta^{18}\text{O}$ ,  $\pm 3\text{‰}$  for  $\delta^2\text{H}$ . Deposits clogging the plate heat exchanger at the Barredo geothermal installation were sampled and studied at the University of Oviedo. X-Ray diffraction of the sample was performed using a D8 Discover X-ray diffractometer. In addition, the sample was studied by reflection-light optical polarizing microscopy in a polished section, and analysed by X-Ray fluorescence, using a portable NITON XL3t 700 detector.

## 4. RESULTS AND DISCUSSION

### 4.1. Hydrochemistry

Table 1 shows the arithmetic mean, maximum and minimum values of obtained field parameters and major/minor ions concentrations. The temperature of Barredo mine water is about  $1^\circ\text{C}$  higher than that of Figaredo mine water, and it increases with depth due to the geothermal gradient (average temperature at Barredo shaft is  $22.3$  and  $22.8^\circ\text{C}$  when pumped at  $100$  and  $200$  m b.g.l, respectively), showing a slight decrease in winter. According to previous data from HUNOSA, the discharge from San José shaft corresponds to a neutral, hard and mineralized water (average electrical conductivity:  $2\text{ mS cm}^{-1}$ ). Its temperature is around  $19^\circ\text{C}$  and its average iron and sulphate contents are  $3.7$  and  $470\text{ mg L}^{-1}$ , reaching up to  $10.9\text{ mg L}^{-1}$  for Fe (Martos, 2014). The average temperature of the Turón River increases  $3^\circ\text{C}$  as a result of introduction of mine water discharge from the San José shaft, which is a quite significant increase. The temperature of the water discharged from Mariana mountain mine, which corresponds to rainwater recently infiltrated, is about  $14^\circ\text{C}$ . Barredo and Figaredo mine waters show negative Eh values (the deeper, the more reducing), whereas the water from Mariana mountain mine, with low residence time, shows oxidizing conditions. All the sampled waters have circumneutral pH. It is slightly higher in Barredo water than in Figaredo water, but no differences with depth have been found. Alkalinity in deep mine waters is high due to the influence of limestone in the sedimentary succession crossed by the mine workings; values are twice that of Mariana water and triple that of river water, so the discharge of mine water into the river increases its alkalinity. All these waters are net

alkaline (Hedin et al., 1994; PIRAMID, 2003; Younger et al., 2002) and their calculated acidity, according to Hedin et al. (1994) is usually zero, excepting in a few Barredo samples reaching up to  $8 \text{ mg L}^{-1} \text{ CaCO}_3$ . According to the categorization proposed by Fichlin et al. (1992), Barredo and Figaredo mine waters can be classified as near neutral, high metal waters, whereas Mariana and Turón River waters are generally near neutral, low metal waters. Not surprisingly, the maximum dissolved oxygen concentration was found in the river water, followed by Mariana, Figaredo and Barredo mine waters. When Barredo water passes through the heat exchanger, it undergoes an average reduction of 23% in its DO.

The total hardness of all the sampled waters is very high (187 to  $677 \text{ mg L}^{-1} \text{ CaCO}_3$ ), except the river water upstream of the mines, which is moderately hard ( $110\text{-}237 \text{ mg L}^{-1} \text{ CaCO}_3$ ) and have high (Barredo and Figaredo waters), medium (Mariana water and river water downstream of San José Mine) and low (river upstream of the mines) volumes of ions in solution. Figaredo water has slightly less dissolved ions than Barredo water, with the difference in values increasing with depth of Barredo sample, which agrees with a longer residence time. Electrical conductivity ranges in deep mine waters between  $2.1$  and  $2.9 \text{ mS cm}^{-1}$ , with an average of  $2.4 \text{ mS cm}^{-1}$ , whereas Mariana water has less ions in solution ( $<1 \text{ mS cm}^{-1}$ ). Analogously, total dissolved solids are ca.  $1,200 \text{ mg L}^{-1}$  in deep mine waters and half as much again in Mariana water, which is in good agreement with their residence time. Turón River water electrical conductivity values double after receiving the mine water discharge, and as a result shows a clear increase in salinity. The mean content of dissolved Fe is slightly higher in Figaredo than in Barredo waters at proximal depths, reaching up to  $3.1$  and  $3.7 \text{ mg L}^{-1}$ , respectively. A maximum concentration of  $5.2 \text{ mg L}^{-1}$  was found in the water pumped from Barredo, but no substantial differences were evident between the average metal contents of waters from each shaft. It can be noted that Fe and Mn contents increase with depth in Barredo shaft. The water from Mariana mine has lower iron concentrations, whilst concentrations in the Turón River increase downstream of San José mine discharge by 5 and 12 times for Fe and Mn. Unfiltered samples contain an average of 50% more Fe and Mn than filtered samples; in particular, these elements seem to be more abundant in the suspended solids of shallow mine waters. Water flowing through the heat exchanger decreases its average Mn content by 11% but its average Fe content increases by 14%, probably because the iron compounds that are clogging the plates are partially redissolved under slightly more reducing conditions. When unfiltered samples are compared, total iron decreases by 62% in the heat exchanger, likely due to the deposition of suspended iron-rich particles.

The chemical reactions by which dissolved iron precipitates in the form of iron (oxy)hydroxides are well documented in the literature (Camden-Smith et al., 2015; Younger et al., 2002, among others). These Fe (oxy)hydroxides occur in anhydrous ( $\text{FeO(OH)}$ ) or hydrated ( $\text{FeO(OH)} \cdot n\text{H}_2\text{O}$ ) forms. The so-called yellow Fe oxide corresponds to the monohydrate or ferric hydroxide ( $\text{Fe(OH)}_3$ ).

According to PHREEQC geochemical modelling, all the sampled waters are sub-saturated in anhydrite, gypsum and Mn (oxy)hydroxides. The saturation index (SI) is lower in Figaredo than in Barredo waters for all species and it decreases with depth in Barredo. Concerning Fe (oxy)hydroxides, all the samples are saturated in hematite and goethite; the highest SI are found in the heat exchanger influent, reaching up to 15.8 and 6.9 for hematite ( $\text{Fe}_2\text{O}_3$ ) and goethite ( $\text{FeO(OH)}$ ), respectively.  $\text{Fe(OH)}_3$  is in equilibrium in all waters excepting those flowing through the heat exchanger, which are slightly saturated in this compound. Deep mine waters are slightly saturated in Fe and Mn carbonates, but these compounds are in equilibrium in Mariana mine and river waters, which are only saturated in hematite and goethite. Ca carbonates show positive SI in all waters, with a maximum value of 1.2 for the heat exchanger influent. The SI found for the minerals are always lower in the effluent than in the influent of the heat exchanger, which agrees with a mineral precipitation on this component.

Additionally, water pumped from Barredo was compared with that flowing through the heat exchanger by means of the Pourbaix (Eh-pH) diagram, which maps out equilibrium phases of an aqueous electrochemical

system (Pourbaix, 1974). These waters have a similar Eh, but the pH is slightly higher in the exchanger. In the Fe-H<sub>2</sub>O system, Barredo water places at the equilibrium line between Fe<sup>2+</sup>(aq) and Fe(OH)<sub>3</sub> (s), so a slight increase of pH favours that the stable phase is the iron hydroxide, producing its precipitation. Therefore, maintaining a water pH of <8 would help avoid Fe oxide precipitation and the clogging associated with it.

Contents of up to 0.17, 1.1 and 2.2 mg L<sup>-1</sup> of Li<sup>+</sup>, F<sup>-</sup>, and Br are present in Barredo and Figaredo waters. These parameters are undetectable, or possibly present in concentrations below the level of analytical resolution, in Mariana and Turón River waters. Significant concentrations of NH<sub>4</sub><sup>+</sup> (up to 0.9 mg L<sup>-1</sup>) were only detected in river waters and indicate some element of leaching from local livestock waste or sewage discharges. There are no significant nitrite or nitrate concentrations in Barredo or Figaredo waters, but in Mariana and the river waters, contents up to 3.0 and 3.6 mg L<sup>-1</sup> of NO<sub>3</sub><sup>2-</sup>, respectively, were found. Phosphate and carbonate ions were not detected in significant concentrations in the sampled waters. The carbon content (both organic and inorganic) in Mariana and river waters is less than half of that of deep mine waters, with Figaredo being slightly lower than Barredo, which is probably related to the greater volume of carbonates encountered in this mine. The highest sulphate concentrations were found in Barredo waters, followed by Figaredo; Mariana and original river waters have low sulphate contents, but river water values increase by 80% post mine water discharge. The effect of mine and river water mixing, evident across several parameters, in the river downstream of the San José mine is more pronounced in the summer, due to lower seasonal river flow. The behaviour of the rest of major ions is better explained by means of a Piper diagram (Fig. 3), which demonstrates that deep mine waters are distinct from Mariana mine and Turón River waters. Both Barredo and Figaredo waters are Na-HCO<sub>3</sub> type and contain a high amount of dissolved ions that increases with sample depth. Conversely, the rest of sampled waters are Ca-HCO<sub>3</sub> type, with Turón River waters having a lower ion in solution than Mariana waters.

#### *Archive results*

Figure 4 shows a comparison of the deep mine water analysis (from Barredo and Figaredo shafts) reported in this paper and existing data representing samples from 2005 to the present (courtesy of HUNOSA; Martos, 2014). Samples taken before mine flooding in 2008 are of Na-HCO<sub>3</sub> water type and they are clearly distinct from those sampled during the flooding period (2008-2009), when they become a more (Ca-Na)-SO<sub>4</sub> type, and after the flooding when water values return to a Na-HCO<sub>3</sub> water (Fig. 4a). Figure 4b shows the time evolution of SO<sub>4</sub> and Fe contents; although there are some sampling gaps, it is evident that sulphate and iron contents increase during the groundwater rebound. This is a well documented trend that is the result of rising water flushing out sulphide oxidation products generated during active mining when mine voids were exposed to atmospheric oxygen. This sudden rise of iron and sulphate contents following post-abandonment flooding, known as “first flush”, was first described by Younger (1997) and Younger (1998). An in-depth theoretical explanation of the first flush is presented in Wolkesdorfer (2008) and Younger (2000) proposes an empirical equation to estimate its duration. It has been described in many mining districts all around the world: Lindsay Colliery, UK (Younger and Banwart, 2001); Montalbion mining area, Australia (Harris et al., 2003); Lorraine basin and Ruhr coal mining district, France-Germany (Blachere et al., 2005), Upper Silesian coal basin, Poland-Czech Republic (Gzyl and Banks, 2007); Chrzanow basin, Poland (Kasprzak and Motyka, 2015), among others. Since the reintroduction of pumping, groundwater rebound has ceased and ion and metal concentrations have demonstrated a gradual decline, indicating water quality recovery to pre-flood levels within ca. 6 years in the case of Barredo-Figaredo mine system.

#### **4.2. Isotopic studies**

Table 2 shows O and H isotopic values, expressed as δ-values against Vienna Standard Mean Ocean Water (VSMOW) standard, for three sampling campaigns from June to November 2015. Duplicate analyses reproduce well within error of reproducibility and the values in the table represent the average value of duplicate results.

8 In 2005, two samples from Figaredo mine were subjected to isotopic analyses in the Zaidín Experimental Station (CSIC, Spain). As the mine was still in operation and pumping was active, waters infiltrated into the galleries of 5th and 8th levels, at depth of 185 and 360 m b.g.l., were sampled.  $\delta^{18}\text{O}$  and  $\delta^2\text{H}$  values ( $-7.33\text{‰}$  and  $-44.8\text{‰}$ ) were practically identical for both samples and they are coherent with those found in the present study. Tritium contents were also determined, obtaining 4.55 and 2.89 UT for the shallow and the deep samples, respectively. According to their tritium content (useful to date young waters), the sampled waters were recent (1.7 and 9.7 years, respectively). Considering the depth of these samples, this means an average velocity of infiltration from the surface of 0.2 m per day.

In Fig. 5,  $\delta^{18}\text{O}$  versus  $\delta^2\text{H}$  is plotted for the present analysis (together with the two samples from 2005). All the mine and river samples fall close to the Global Mean Meteoric Water Line (GMWL), indicating their close relationship to meteoric water through direct and rapid infiltration, in the absence of evaporative loss (which would push samples far to the right of the GMWL plot) or processes of ionic exchange with host rocks (Domenico and Schwartz, 1998). The surface waters, especially for the Mariana mine, show slightly heavier isotopic values as compared to deep mine waters. The rapidly percolating waters from the Mariana mine may better represent modern rainwater values under warmer summer-type conditions when evaporation of heavier isotopes of O and H into the atmosphere is easier to accomplish. If this is the case, then the lighter isotopic values of the deeper mine waters may represent a more composite yearly or long-term isotopic average for the area. Further sampling and analysis of samples over 12 months, to separate out any seasonal variation, will have to be carried out to know for certain if this is the case. Rainfall samples fall close to the GMWL and they represent a good approximation of the isotopic composition of the local rainfall that recharges the river and mine systems. The age of the mine waters that are currently pumped from the flooded reservoir is unknown; however, considering the previous data, we could provisionally conclude that the  $\delta^{18}\text{O}$  and  $\delta^2\text{H}$  composition of the rainfall has not changed significantly since 2005, as the effects that cause isotopic division (i.e. altitude, latitude and distance to the coast) have remained constant over the last decade.

In some particular campaigns, mixed mine water appears in alignment with those waters from which it is sourced (i.e. mine water values fall between local rainfall and river water), but this is not a typical trend. In general, no significant differences between different sampling depths were found in the case of these isotopes, and all the deep mine waters appear grouped together. Also, little difference has so far been observed between samples taken in summer and winter months.

#### 4.3. Analysis of deposits on the heat exchanger

Mine water TDS is higher than desirable for optimal heat exchanger performance. The solubility of dissolved minerals is affected by changes in temperature within the heat exchanger and chemical reactions between compounds found in the water. In particular, the iron content and hardness of the water are largely responsible for the precipitation of Fe (oxy)hydroxides on the heat exchanger (Fig. 6a). The origin of common iron compounds in coal mine water are well known: pyrite oxidation generates  $\text{Fe}^{2+}$  which undergoes oxidation, releasing  $\text{Fe}^{3+}$ , and if Eh/pH are adequate, the ferric ion precipitates as ferric hydroxide ( $\text{Fe}(\text{OH})_3$ ) (Camden-Smith et al., 2015). As it was previously stated, a pH increase nudges the chemical reaction equilibrium in favor of ferric hydroxide precipitation. The effect of temperature, in  $K_{\text{eq}}$  of this reaction is difficult to specify, as ferric oxyhydroxide can take a number of forms (amorphous, microcrystalline), but Appelo and Postma (1996) suggest an absolute value of:  $K_{\text{eq}} = 10^{-4}$ . In this case, the temperature of the influent is slightly decreases after flowing through the exchanger, but the effect of the pH (a “master variable”) increase is more critical than that of the temperature.

X-Ray fluorescence and optical microscopy studies showed that the precipitates sampled on the exchanger are mainly amorphous iron oxy-hydroxides, containing up to 6.3% of  $\text{CaCO}_3$  and minor concentrations of Mn oxide. Only a minimal portion of crystalline goethite [ $\alpha\text{-FeO}(\text{OH})$ ], was identified by X-Ray diffraction. When



observed by optical polarizing microscopy, the major constituent of the heat exchanger deposits is a grey/brown non-crystalline layered soft component (Fig. 6b), which is an iron oxide. Goethite is common but not frequent; it appears in individual grains of irregular morphology and shows marked colloform internal textures and a grain size up to 200-300  $\mu\text{m}$  (Fig. 6c). Dispersed subangular, well preserved pyrite grains 20-50  $\mu\text{m}$  in size are present as individual particles. These differ from the above minerals because they do not originate by precipitation from the mine water and are likely to have been transported in suspension to the sampling point (Fig. 6d). These particles are a component of the suspended solids captured during the precipitation process (a Scanning Electron Microscope analysis would confirm this). This result is in agreement with the reduction of Fe content in unfiltered samples after passing through the heat exchanger. Therefore, we suggest water filtering and regular cleaning of the heat exchanger will be sufficient to keep the fluid velocity high enough to inhibit scaling and clogging.

Additional strategies could be used to aid reduction of iron precipitation and clogging, including: avoiding water exposure at to atmospheric oxygen, avoiding water level oscillations inside the mine reservoir, keeping the pumped mine water under pressure, stablishing a closed loop so the mine water does not come in direct contact with the heat exchangers, using phropylactic heat exchangers, and adding environmentally benign (bio)chemical reducing agents (i.e. sodium dithionite) that maintain the iron in its ferrous form. (Banks, 2012).

## 5. CONCLUSIONS

The Barredo and Figaredo mines are interconnected so their waters are hydrochemically analogous, with temperature and the concentration of dissolved ions slightly lower in Figaredo. They are both of  $\text{Na-HCO}_3$  water type and they are alkaline, near neutral, high metal, very hard, contain high values of ions in solution, demonstrate reducing conditions, and have relatively high carbon content. Temperature, salinity, ionic and metal content generally increase with depth in Barredo. Like in other documented flooded mines, during the flooding period (2008-2009), Barredo-Figaredo waters changed to a  $(\text{Ca-Na})\text{-SO}_4$  type; sulphate and iron contents increased during the groundwater rebound, as water washed out the sulphide oxidation products generated when the mine was active, but after the flooding, these concentrations gradually recovered to the original values.

Water discharged from Mariana mountain mine is completely different to that pumped from the underground mines. Its temperature, alkalinity, metal and ionic content is much lower, and its DO content is higher. Like the river water, it is of  $\text{Ca-HCO}_3$  type. Ammonium species were only found in Turón River water, which increases its temperature, alkalinity, electrical conductivity, sulphate and metal content after receiving discharge from pumped mine workings. River water quality deteriorates when it is mixed with mine water, and this effect is more pronounced in the summer, due to the lower river flow.

Studies of the  $\text{H}_2\text{O}$  isotopes indicate that sampled waters are close to recent meteoric waters. In the case of mine waters, this is compatible with a direct and rapid infiltration. This is in agreement with previous studies, but further investigation is required.

The temperature of Barredo –Figaredo water is stable ( $22^\circ\text{C}$  when pumped at 100 m b.g.l) and a flow above  $100 \text{ L}\cdot\text{s}^{-1}$  (corresponding to the recharge of the reservoir) can be guaranteed. The relative stability of the studied parameters suggests that these waters represent a dependable thermal resource that, given current levels of demand, can be sustainably exploited for long-term geothermal use. However, it must be cautioned that the hardness and iron content of these waters can cause clogging problems in pipes and, in particular, in heat exchangers. At the Barredo geothermal installation, precipitates of iron oxy-hydroxides, deposits of previously suspended pyrite particles and some scaling were observed on the plate heat exchanger, so regular maintenance is required in order to maintain optimal system performance. Broadly, monitoring mine water chemistry (in particular key parameters such as temperature, pH, Eh, Fe, Mn, Ca, Mg, or  $\text{SO}_4$ ) is essential for efficient management and guaranteeing the sustainability of mine water heat pump schemes. Analysis of

deposits causing clogging can reveal useful information, such as their origin (dissolved or suspended solids in the water), and help to develop optimal strategies to retard precipitation in pipes and heat exchangers. Strategies such as avoiding water level fluctuation and water aeration, as well as the addition of reducing agents can all help to inhibit clogging in mine geothermal installations.

## 6. ACKNOWLEDGMENTS

This work was funded as part of the Low-Carbon After-Life (LoCAL) project under the European Commission Research Fund for Coal and Steel (RFCR-CT-2014-00001). Isotopic analysis was carried out by Adrian Boyce and Alison McDonald at the NERC supported ICSF within the SUERC (NERC Facility contract F14/G6/11/01).

## 7. REFERENCES

- Aller, J., Gallastegui, J., 1995. Analysis of kilometric-scale superposed folding in the Central Coal basin (Cantabrian Zone, NW Spain). *J. Struct. Geol.* 17(7), 961-969. DOI: 10.1016/0191-8141(94)00115-G.
- Alonso, J.L., Pulgar, J., García-Ramos, J.C., Barba, P., 1996. Tertiary basins and alpine tectonics in the Cantabrian Mountains (NW Spain), in: Friend, P. F., Dabrio, C. J.(Eds.), *Tertiary Basins of Spain*. Cambridge University Press, Cambridge, pp. 214-227.
- Andrés, C., Ordóñez, A., Álvarez, R., 2015. Hydraulic and Thermal Modelling of an Underground Mining Reservoir. *Mine Water Environ.* DOI: 10.1007/s10230-015-0365-1.
- Appelo, C.A.J., Postma, D., 1996. *Geochemistry, groundwater and pollution*. Balkema, Rotterdam.
- Banks, D., 2012. *An introduction to thermogeology: ground source heating and cooling*, second ed. John Wiley & Sons, Chichester (UK).
- Banks, D., 2016. Making the red one green: renewable heat from abandoned flooded mines, in: IAH (Irish Group) (Ed.), *Proceedings of the 36th Annual Groundwater Conference of the International Association of Hydrogeologists*. Tullamore, County Offaly, Ireland, pp. 1-9.
- Blachere, A., Metz, M., Rengers, R., Eckart, M., Klinger, C., Unland, W., 2005. Evaluation of mine water quality dynamics in complex large coal mine fields, in: Loredó, P., Pendás, F. (ed.), *Proceedings of the 9<sup>th</sup> International Mine Water Congress*, Oviedo, Spain, pp. 551-557.
- Blöcher, M.G., Zimmermann, G., Moeck, I., Brandt, W., Hassanzadegan, A., Magri, F., 2010. 3D numerical modelling of hydrothermal processes during the lifetime of a deep geothermal reservoir. *Geofluids* 10, 406–421. DOI: 10.1111/j.1468-8123.2010.00284.x.
- Burnside, N.M., Banks, D., Boyce, A.J., 2016a. Sustainability of thermal energy production at the flooded mine workings of the former Caphouse Colliery, Yorkshire, United Kingdom. *Int. J. Coal Geol.* DOI: 10.1016/j.coal.2016.03.006.
- Burnside, N.M., Banks, D., Boyce, A.J., Athresh, A., 2016b. Hydrochemistry and stable isotopes as tools for understanding the sustainability of thermal energy production from a ‘standing column’ heat pump system: Markham Colliery, Bolsover, Derbyshire, UK. *Int. J. Coal Geol.* 165, 223-265. DOI: 10.1016/j.coal.2016.08.021.
- Butterworth, D., 2002. Design of shell-and-tube heat exchangers when the fouling depends on local temperature and velocity. *Appl. Therm. Eng.* 22, 789–801. DOI: 10.1016/S1359-4311(02)00025-X.
- Camden-Smith, B., Johnson, R.H., Camden-Smith, P., Tutu, H., 2015. Geochemical modelling of water quality and solutes transport from mining environments, in: Lee, T.S. (Ed.), *Research and practices in water quality*, pp. 39-64. DOI: 10.5772/59234. <http://www.intechopen.com/books/research-andpractices-in-water->

[quality/geochemical-modelling-of-water-quality-and-solutes-transport-from-miningenvironments](#) (accessed 11.09.2016).

Domenico, P.A., Schwartz, F.W., 1998. Physical and chemical hydrogeology, second ed. John Wiley & Sons, New York.

Fichlin, W.H., Plumlee, G.S., Smith, K.S., Mchugh, J.B., 1992. Geochemical classification of mine drainage and natural drainage in mineralized areas, in: Kharaka, Y.K., Maest, A.S. (Eds.), Proceedings of 7<sup>th</sup> international symposium on water-rock interaction, Rotterdam, pp 381–384.

García-Loygorri, A., Ortuño, G., Caride, C., Gervilla, M., Greber, C., Feys, R., 1971. El Carbonífero en la cuenca central asturiana. *Trabajos de Geología* 3, 101-150.

Garrido, E.A., García-Gil, A., Vázquez-Suñe, E., Sánchez-Navarro, J., 2016. Geochemical impacts of groundwater heat pump systems in an urban alluvial aquifer with evaporitic bedrock. *Sci. Total Environ.* 544, 354–368. DOI:10.1016/j.scitotenv.2015.11.096.

Gzyl, G., Banks, D., 2007. Verification of the “first flush” phenomenon in mine water from coal mines in the Upper Silesian Coal Basin, Poland. *J. Contam. Hydrol.* 92, 66–86. DOI: 10.1016/j.jconhyd.2006.12.001.

Hall, A., Scott, J.A., Shang, H., 2011. Geothermal energy recovery from underground mines. *Renew. Sust. Energ. Revs.* 15, 916–924. DOI: 10.1016/j.rser.2010.11.007.

Hamm, V., Bazargan, B., 2010. Modelling of fluid flow and heat transfer to assess the geothermal potential of a flooded coal mine in Lorraine, France. *Geothermics* 39, 177–186. DOI: 10.1016/j.geothermics.2010.03.004.

Harris, D.L., Lottermoser, B.G., Duchesne, J., 2003. Ephemeral acid mine drainage at the Montalbion silver mine, north Queensland. *Aust. J. Earth Sci.* 50, 797–809. DOI: 10.1111/j.1440-0952.2003.01029.x.

Hedin, R.S., Nairn, R.W., Kleinmann, R.L.P., 1994. Passive treatment of polluted coal mine drainage. Bureau of Mines Information Circular 9389. <http://www.arcc.osmre.gov/resources/impoundments/BoM-IC-9389-PassiveTreatmentofCoalMineDrainage-Hedinetal1993.pdf> (accessed 12.09.2016).

Janson, E., Boyce, A., Burnside, N., Gzyl, G., 2016. Preliminary investigation on temperature, chemistry and isotopes of mine water pumped in Bytom geological basin (USCB Poland) as a potential geothermal energy source. *Int. J. Coal Geol.* DOI: 10.1016/j.coal.2016.06.007.

Jardón, S., Ordóñez, A., Álvarez, R., Cienfuegos, P., Loredó, J., 2013. Mine water for energy and water supply in the Central Coal Basin of Asturias (Spain). *Mine Water Environ.* 32, 139–151. DOI: 10.1007/s10230-013-0224-x.

Kasprzak, A., Motyka, J., 2015. The influence of the “Trzebionka” mine flooding for changes in groundwater chemistry of triassic aquifer. *Prz. Geol.* 63, 805–809.

Loredó, C., Roqueñí, N., Ordóñez, A., 2016. Modelling flow and heat transfer in flooded mines for geothermal energy use: A review. *Int. J. Coal Geol.* DOI: 10.1016/j.coal.2016.04.013.

Martos, E., 2014. Caracterización hidrogeológica de la Cuenca del río Turón (Asturias) en relación con la clausura de explotaciones mineras de carbón. Unpublished PhD Thesis. University of Oviedo, Spain, 334p.

MTS Systems Corporation, 2005. Heat exchanger care and water quality guide. Manual Part No. 015- 164-000 C. Minnesota, USA, 22 p. [https://www.mts.com/ucm/groups/public/documents/library/mts\\_004900.pdf](https://www.mts.com/ucm/groups/public/documents/library/mts_004900.pdf) (accessed 22.08.2016).

- Nelson, S.T., 2000. A simple, practical methodology for routine VSMOW/SLAP normalization of water samples analyzed by continuous flow methods. *Rapid Commun. Mass Spectrom.* 14, 1044–1046. DOI:10.1002/1097-0231(20000630)14:12<1044::AID-RCM987>3.0.CO;2-3.
- Ordóñez, A., Jardón, S., Álvarez, R., Andrés, C., Pendás, F., 2012. Hydrogeological definition and applicability of abandoned coal mines as water reservoirs. *J. Environ. Monit.* 14, 2127–2136. DOI: 10.1039/c2em11036a.
- Ozyurt, N.N., Lutz, H.O., Hunjak, T., Mance, D., Roller-Lutz, Z., 2014. Characterization of the Gacka River basin karst aquifer (Croatia): Hydrochemistry, stable isotopes and tritium-based mean residence times. *Sci. Total Environ.* 487, 245–254. DOI:10.1016/j.scitotenv.2014.04.018.
- Parkhurst D.L., Appelo C.A.J., 1999. User's guide to PHREEQC (Version 2). A computer program for speciation, batch-reaction, one-dimensional transport, and inverse geochemical calculations. U.S. Geological Survey. Water-Resources Investigations Report 99-4259.  
ftp://brrftp.cr.usgs.gov/pub/charlton/phreeqc/Phreeqc\_2\_1999\_manual.pdf (accessed 24.08.2016).
- Peralta, E., Breede, K., Falcone, G., 2015. Geothermal heat recovery from abandoned mines: a systematic review of projects implemented worldwide and a methodology for screening new projects. *Environ. Earth Sci.* 73, 6783–6795. DOI: 10.1007/s12665-015-4285-y.
- Piedad-Sánchez, N., Izart, A., Martínez, L., Suárez-Ruiz, I., Elie, M., Menetrier, C., 2004. Paleothermicity in the Central Asturian coal basin, North Spain. *Int. J. Coal Geol.* 58, 205–229. DOI: 10.1016/j.coal.2004.02.001.
- PIRAMID Consortium, 2003. Engineering guidelines for the passive remediation of acidic and/or metalliferous mine drainage and similar wastewaters. <http://www.imwa.info/piramid/files/PIRAMIDGuidelinesv10.pdf> (accessed 12.09.2016).
- Pourbaix, M., 1974,. Atlas of electrochemical equilibria in aqueous solutions, second English ed. National Association of Corrosion Engineers. Houston, Texas.
- Preene, M., Younger, P.L., 2014. Can you take the heat? – Geothermal energy in mining. *Min. Technol.* 123, 107–118. DOI:10.1179/1743286314Y.0000000058.
- Raymond, J., Therrien, R., 2007. Low-temperature geothermal potential of the flooded Gaspé Mines, Québec, Canada. *Geothermics* 37, 189–210. DOI:10.1016/j.geothermics.2007.10.001.
- Raymond, J., Therrien, R., Gosselin, L., Lefebvre, R., 2011. Numerical analysis of thermal response test with a groundwater flow and heat transfer model. *Renew Energy* 36(1), 315–324. DOI: 10.1016/j.renene.2010.06.044.
- Renz, A., Rühaak, W., Schätzl, P., Diersch, H.J.G., 2009. Numerical modelling of geothermal use of mine water: Challenges and examples. *Mine Water Environ.* 28, 2–14. DOI: 10.1007/s10230-008-0063-3.
- Uhlík, J., Baier, J., 2012. Model evaluation of thermal energy potential of hydrogeological structures with flooded mines. *Mine Water Environ.* 31, 179–191. DOI: 10.1007/s10230-012-0186-4.
- Watzlaf, G.R., Ackman, T.E., 2006. Underground mine water for heating and cooling using geothermal heat pump systems. *Mine Water Environ.* 25, 1–14. DOI: 10.1007/s10230-006-0103-9.
- Wolkersdorfer, C., 2008. Water management at abandoned flooded underground mines: fundamentals, tracer test, modelling, water treatment. Springer, Heidelberg, Germany.
- Younger, P.L., 2000. Predicting temporal changes in total iron concentrations in groundwaters flowing from abandoned deep mines: a first approximation. *J. Contam. Hydrol.* 44, 47–69. DOI: 10.1016/S0169-7722(00)00090-5.

Younger, P.L., Banwart, S.A., 2002. Time-scale issues in the remediation of pervasively-contaminated groundwaters at abandoned mine sites. Groundwater quality: natural and enhanced restoration of groundwater pollution, in: IAHS (Ed.) Proceedings of the Groundwater Quality 2001 Conference. Publ. no. 275, Sheffield, UK, pp. 585-591.

Younger, P.L., 1997. The longevity of mine water pollution: a basis for decision-making. Sci. Total Environ. 194/195, 457–466. DOI: 10.1016/S0048-9697(96)05383-1.

Younger, P.L., 1998. Coalfield abandonment: geochemical processes and hydrochemical products, in: Nicholson, K. (ed.), Energy and the environment: geochemistry of fossil, nuclear & renewable resources. Environmental Geochemistry Series Vol. 1, MacGregor Science, pp. 1-29.

Younger, P.L., Banwart, S.A., Hedin, R.S., 2002. Mine water, Hydrology, Pollution, Remediation. Kluwer Academic Publishers, Dordrecht, The Netherlands.

Table 1. Summary of analytical results of 7 sampling campaigns (Jan'15-Feb'16), taking water from Barredo (pumped at 100 and 200 m of depth), Figaredo and Mariana mines, as well as the Turón River and the heat exchanger in the Barredo geothermal system. All in mg·L<sup>-1</sup> except Temperature (°C), ORP (mV) and electrical conductivity (μS·cm<sup>-1</sup>). (\*) Data from Martos (2014)

|   |      | Temperature | Eh    | pH  | DO  | El. cond. | Hardness | TDS   | Alkalinity | Mn   | Fe   | NH <sub>4</sub> <sup>+</sup> | Ca <sup>2+</sup> | Mg <sup>2+</sup> | Na <sup>+</sup> | K <sup>+</sup> | HCO <sub>3</sub> <sup>-</sup> | SO <sub>4</sub> <sup>2-</sup> | Cl <sup>-</sup> | NO <sub>3</sub> <sup>2-</sup> | TC   | IC   | TOC |
|---|------|-------------|-------|-----|-----|-----------|----------|-------|------------|------|------|------------------------------|------------------|------------------|-----------------|----------------|-------------------------------|-------------------------------|-----------------|-------------------------------|------|------|-----|
| Barredo mine water (100 m)                | mean | 22.3        | -35.1 | 7.9 | 2.6 | 2,416     | 571      | 1,220 | 1,057      | 0.79 | 1.09 | 0.0                          | 119              | 65.6             | 431             | 7.8            | 987                           | 624                           | 15.1            | 0.0                           | 203  | 195  | 8.3 |
|   | max. | 22.9        | -5.67 | 8.4 | 4.6 | 2,886     | 648      | 1,443 | 1,147      | 5.20 | 3.70 | 0.0                          | 144              | 69.0             | 534             | 9.7            | 1,159                         | 686                           | 18.8            | 0.0                           | 241  | 231  | 21  |
|   | min. | 21.6        | -78.7 | 7.4 | 1.5 | 2,102     | 495      | 1,051 | 921        | 0.10 | 0.00 | 0.0                          | 90.1             | 62.3             | 392             | 6.7            | 881                           | 570                           | 12.9            | 0.0                           | 175  | 166  | 2.0 |
| Barredo mine water (200m)                 | mean | 22.8        | -52.2 | 7.8 | 2.9 | 2,438     | 595      | 1,389 | 1,160      | 1.05 | 1.56 | 0.0                          | 126              | 67.4             | 455             | 7.5            | 1031                          | 651                           | 14.4            | 0.0                           | 203  | 196  | 7.5 |
|   | max. | 23.3        | -21.6 | 8.2 | 5.0 | 2,943     | 659      | 2,294 | 1,519      | 3.50 | 4.30 | 0.0                          | 142              | 73.1             | 583             | 8.5            | 1,218                         | 722                           | 16.5            | 0.0                           | 244  | 223  | 22  |
|   | min. | 22.4        | -98.5 | 7.3 | 1.5 | 2,126     | 518      | 1,064 | 982        | 0.10 | 0.00 | 0.0                          | 95.6             | 62.1             | 404             | 6.8            | 931                           | 592                           | 13.1            | 0.0                           | 164  | 166  | 0.4 |
| Plate heat exchanger influent             | mean | 22.1        | -34.2 | 8.2 | 3.3 | 2,429     | 535      | 1,260 | 1,034      | 1.81 | 1.20 | 0.0                          | 105              | 65.2             | 445             | 7.0            | 974                           | 626                           | 14.8            | 0.0                           | 180  | 175  | 6.9 |
|   | max. | 22.9        | -2.30 | 8.9 | 4.6 | 2,832     | 644      | 1,416 | 1,092      | 5.10 | 3.30 | 0.0                          | 138              | 71.8             | 543             | 7.3            | 1,155                         | 689                           | 16.2            | 0.0                           | 231  | 224  | 20  |
|   | min. | 20.8        | -66.2 | 7.6 | 2.0 | 2,134     | 407      | 1,198 | 909        | 0.00 | 0.00 | 0.0                          | 54.7             | 62.0             | 414             | 6.7            | 811                           | 569                           | 14.1            | 0.0                           | 126  | 123  | 2.1 |
| Plate heat exchanger effluent             | mean | 20.3        | -37.1 | 8.1 | 2.6 | 2,471     | 543      | 1,279 | 1,057      | 1.62 | 1.41 | 0.0                          | 111              | 63.6             | 462             | 7.2            | 970                           | 627                           | 14.2            | 0.0                           | 197  | 192  | 7.0 |
|   | max. | 22.9        | -6.20 | 8.7 | 4.7 | 2,888     | 623      | 1,444 | 1,171      | 4.80 | 4.00 | 0.0                          | 144              | 64.2             | 542             | 7.9            | 1,160                         | 689                           | 16.2            | 0.0                           | 236  | 223  | 20  |
|   | min. | 17.1        | -68.1 | 7.5 | 0.1 | 2,268     | 343      | 1,202 | 738        | 0.00 | 0.00 | 0.0                          | 31.4             | 63.1             | 410             | 6.9            | 659                           | 579                           | 12.8            | 0.0                           | 128  | 127  | 0.6 |
| Figaredo mine water (100 m)               | mean | 21.6        | -47.8 | 7.6 | 3.2 | 2,324     | 588      | 1,162 | 1,051      | 0.40 | 1.60 | 0.0                          | 136              | 59.7             | 270             | 5.3            | 751                           | 495                           | 12.8            | 0.0                           | 148  | 145  | 3.1 |
|   | max. | 22.2        | -46.2 | 8.1 | 3.8 | 2,354     | 677      | 1,177 | 1,110      | 0.60 | 3.10 | 0.0                          | 153              | 70.8             | 413             | 6.7            | 997                           | 646                           | 14.6            | 0.0                           | 194  | 189  | 5.2 |
|   | min. | 21.2        | -49.4 | 7.1 | 2.9 | 2,300     | 456      | 1,150 | 1,019      | 0.10 | 0.10 | 0.0                          | 114              | 41.3             | 29.8            | 3.1            | 314                           | 232                           | 9.89            | 0.0                           | 62.8 | 59.9 | 1.2 |
| Mariana mountain mine water               | mean | 14.2        | 27.0  | 7.9 | 4.7 | 958       | 480      | 509   | 504        | 0.67 | 0.17 | 0.0                          | 117              | 44.9             | 109             | 3.9            | 446                           | 306                           | 9.86            | 1.2                           | 91.0 | 88.1 | 5.0 |
|   | max. | 14.8        | 72.8  | 8.8 | 5.5 | 1,125     | 580      | 562   | 811        | 3.60 | 0.70 | 0.2                          | 156              | 66.3             | 428             | 7.2            | 779                           | 640                           | 13.4            | 3.0                           | 144  | 149  | 9.5 |
|   | min. | 13.0        | 3.21  | 7.2 | 3.9 | 823       | 370      | 412   | 372        | 0.00 | 0.00 | 0.0                          | 62.5             | 32.9             | 16.2            | 2.7            | 271                           | 164                           | 8.19            | 0.0                           | 54.1 | 51.3 | 2.8 |
| Turón River (upstream of mines)           | mean | 12.9        | 38.5  | 8.2 | 5.6 | 431       | 189      | 302   | 289        | 0.06 | 0.02 | 0.3                          | 53.2             | 13.3             | 22.9            | 2.5            | 214                           | 45.4                          | 7.42            | 1.9                           | 47.1 | 41.7 | 5.4 |
|   | max. | 14.8        | 63.7  | 8.3 | 7.0 | 528       | 237      | 406   | 317        | 0.31 | 0.10 | 0.8                          | 65.5             | 17.6             | 31.3            | 3.8            | 259                           | 66.3                          | 10.4            | 3.1                           | 54.7 | 50.1 | 7.3 |
|   | min. | 12.1        | 10.0  | 8.0 | 4.1 | 274       | 110      | 199   | 235        | 0.00 | 0.00 | 0.0                          | 32.6             | 6.77             | 8.62            | 1.0            | 116                           | 26.4                          | 6.08            | 1.0                           | 30.5 | 23.5 | 4.0 |
| San José mine discharge (*)               | mean | 18.9        |       | 7.1 | 7.0 | 2,052     | 538      |       |            | 0.7  | 3.7  |                              | 100              | 69.3             | 197             | 8.8            | 591                           | 472                           | 12.1            | 0.7                           |      |      |     |
|   | max. | 19.9        |       | 7.7 | 7.4 | 3,040     | 550      |       |            | 1.2  | 10.9 |                              | 120              | 78.0             | 417             | 13             | 810                           | 803                           | 18.0            | 2.0                           |      |      |     |
|   | min. | 16.6        |       | 6.6 | 6.6 | 1,584     | 522      |       |            | 0.3  | 0.3  |                              | 87               | 60.0             | 103             | 5.0            | 378                           | 296                           | 10.0            | 0.0                           |      |      |     |
| Turón River (downstream of San José mine) | mean | 16.0        | 39.7  | 8.1 | 6.0 | 866       | 352      | 557   | 417        | 0.74 | 0.10 | 0.2                          | 85.3             | 33.3             | 71.4            | 3.8            | 364                           | 245                           | 10.3            | 2.4                           | 66   | 62.8 | 3.6 |
|   | max. | 19.0        | 53.5  | 8.3 | 6.3 | 1,649     | 578      | 824   | 671        | 2.60 | 0.30 | 0.9                          | 131              | 59.8             | 206             | 7.2            | 655                           | 631                           | 22.4            | 3.6                           | 124  | 120  | 6.0 |
|   | min. | 13.0        | 24.0  | 7.9 | 5.3 | 436       | 187      | 338   | 196        | 0.10 | 0.00 | 0.0                          | 49.8             | 15.0             | 20.1            | 1.5            | 179                           | 65.7                          | 6.10            | 0.0                           | 41.6 | 35.5 | 2.0 |

Table 2. O and H isotope of H<sub>2</sub>O in the sampled waters

| Sample  | Date           | $\delta^{18}\text{O}_{\text{VSMOW}} (\text{‰})$ | $\delta^2\text{H}_{\text{VSMOW}} (\text{‰})$ |
|---|----------------|---|--|
| Barredo mine water (pumped at 100 m of depth)         | June 2015      | -7.4  | -44.2  |
|   | September 2015 | -7.1  | -44.0  |
|   | November 2015  | -7.3  | -46.6  |
| Barredo mine water (pumped at 200 m of depth)         | June 2015      | -7.4  | -44.3  |
|   | September 2015 | -7.3  | -45.1  |
|   | November 2015  | -7.4  | -46.3  |
| Barredo mine water (pumped at 100 and 200 m of depth) | June 2015      | -7.4  | -45.5  |
|   | September 2015 | -7.4  | -46.0  |
| Figaredo mine water                                   | June 2015      | -7.5  | -46.7  |
|   | September 2015 | -7.5  | -47.9  |
| Mariana mountain mine water                           | June 2015      | -7.2  | -42.2  |
|   | September 2015 | -7.1  | -42.4  |
|   | November 2015  | -7.2  | -41.9  |
| Turón river (upstream of the mines)                   | June 2015      | -7.7  | -44.1  |
|   | September 2015 | -7.2  | -41.1  |
|   | November 2015  | -7.5  | -44.3  |
| Turón river (downstream of San José mine)             | June 2015      | -7.4  | -44.6  |
|   | September 2015 | -7.6  | -45.8  |
|   | November 2015  | -7.6  | -47.0  |

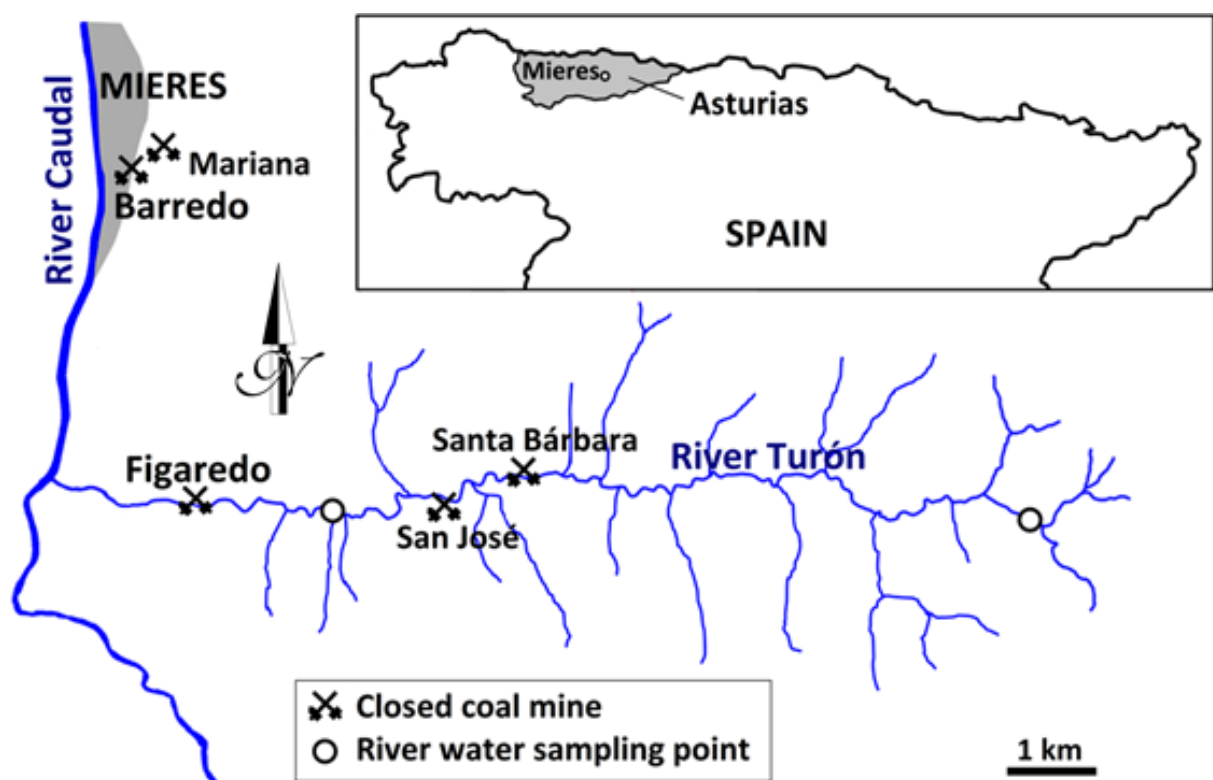


Fig. 1. Location of the studied area: closed mines and sampling points



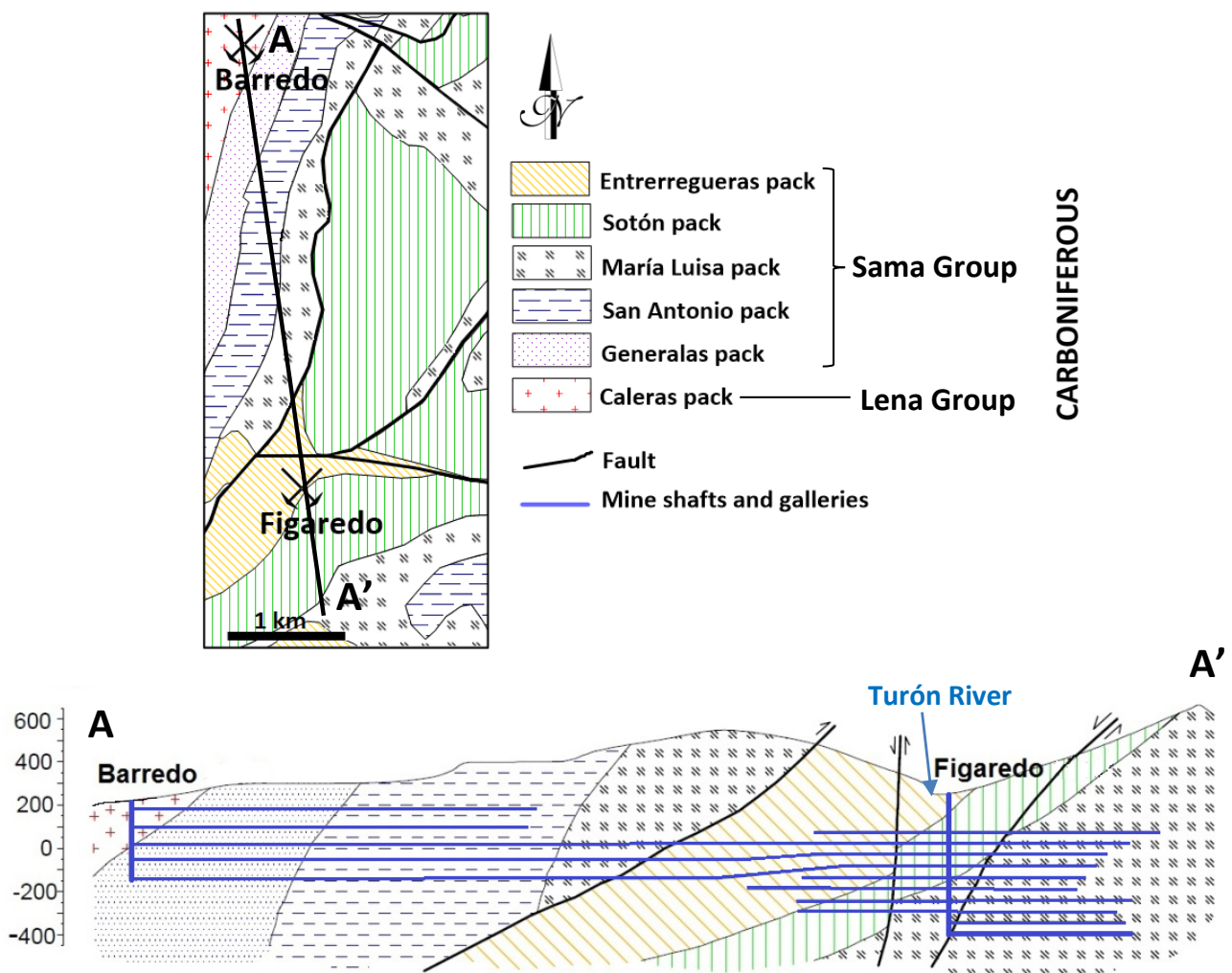


Fig. 2. Geological map and cross section across the Barredo and Figaredo shafts

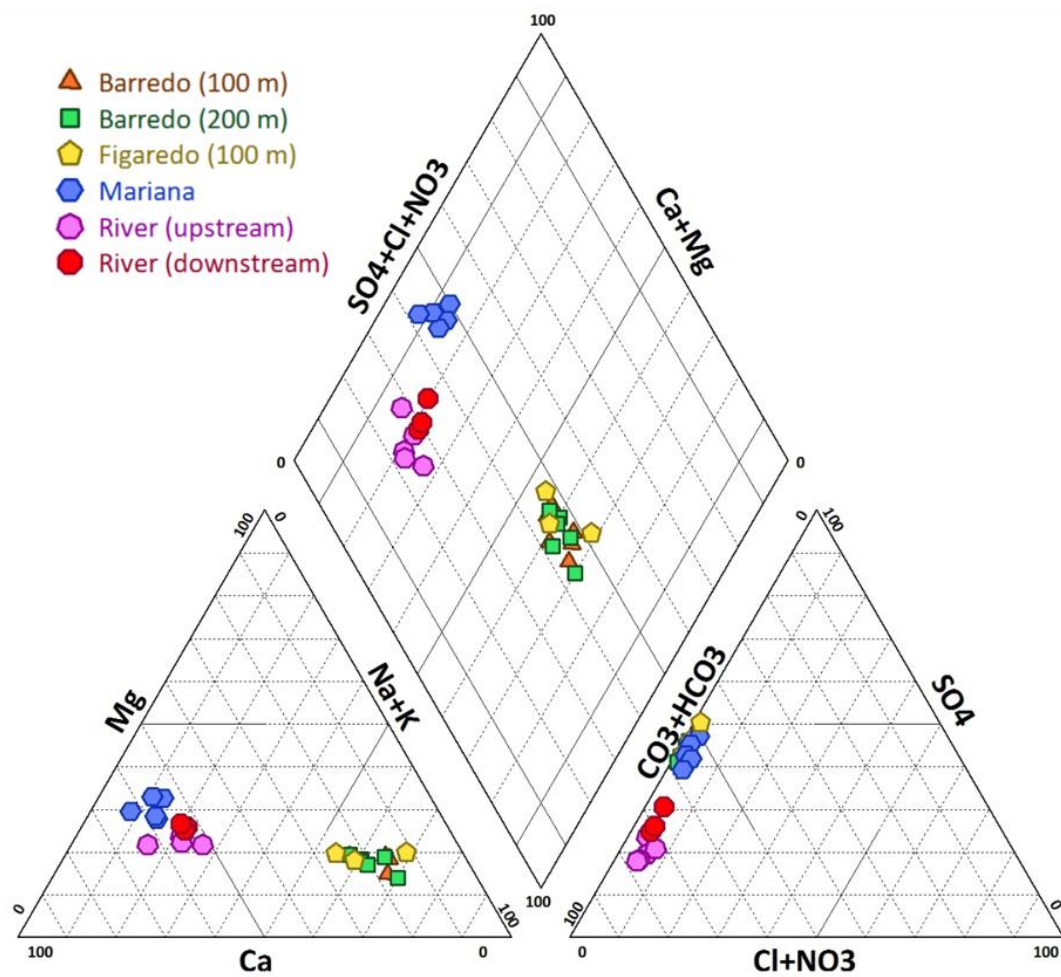


Fig. 3. Piper diagram showing the different waters sampled for this study from 2015-2016

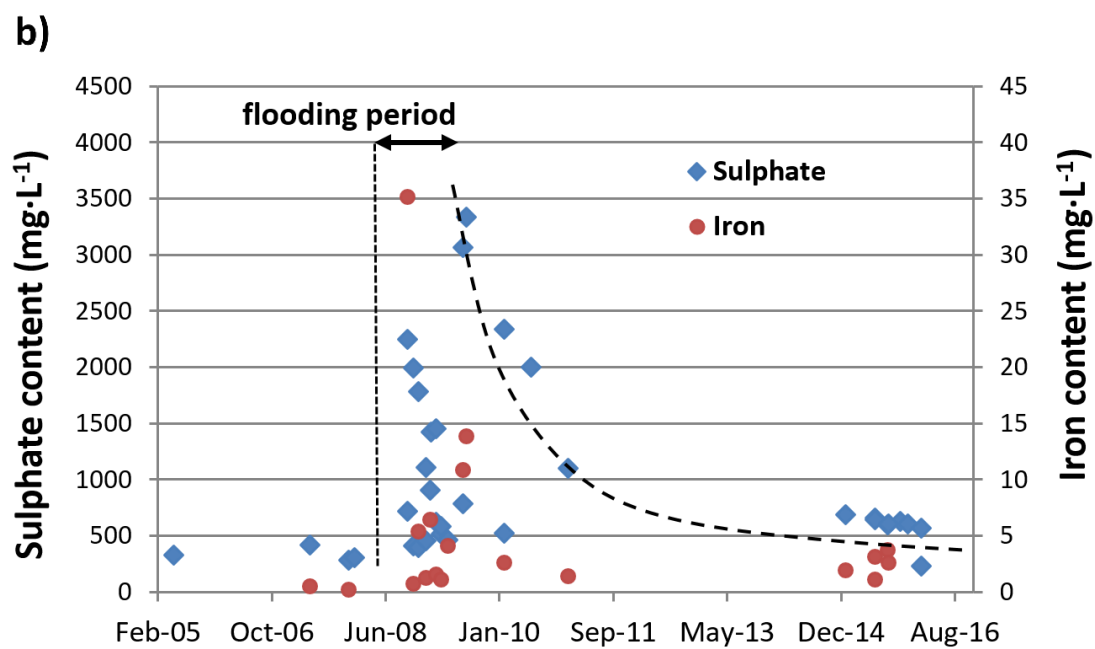
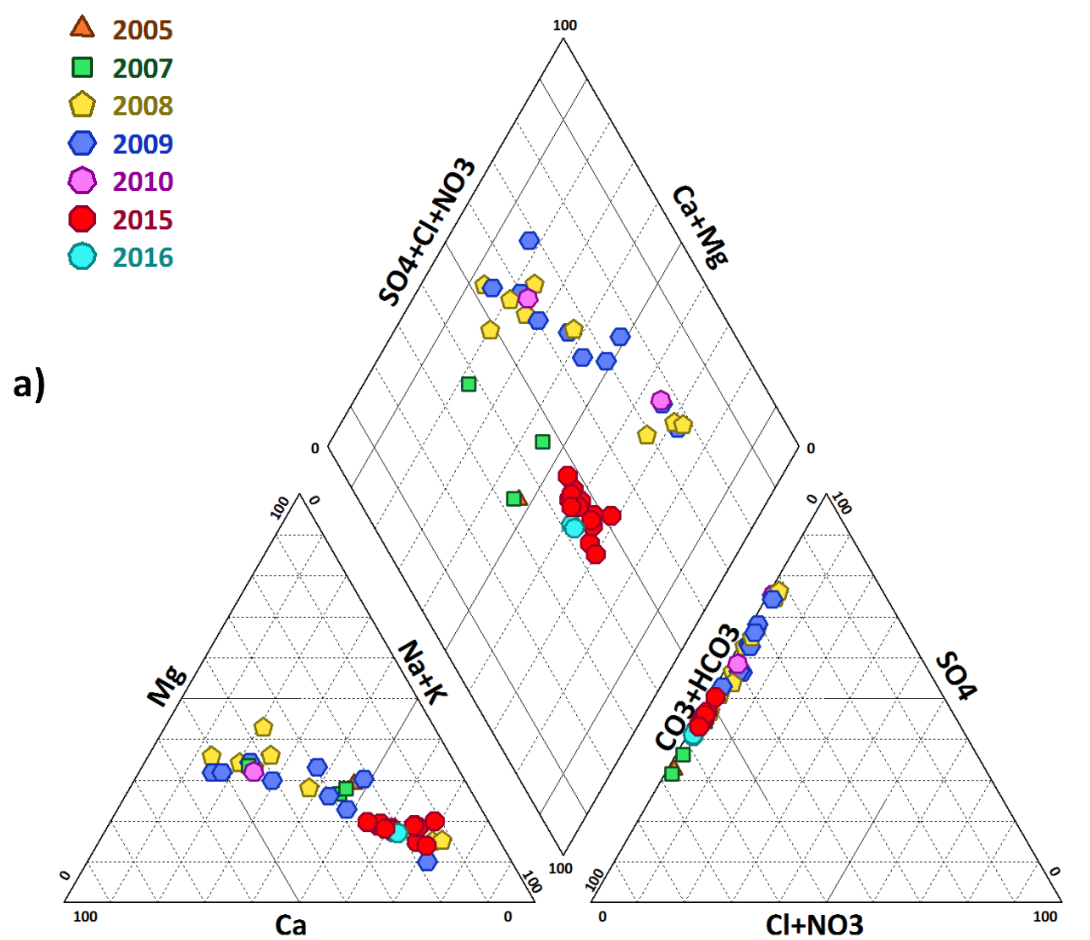
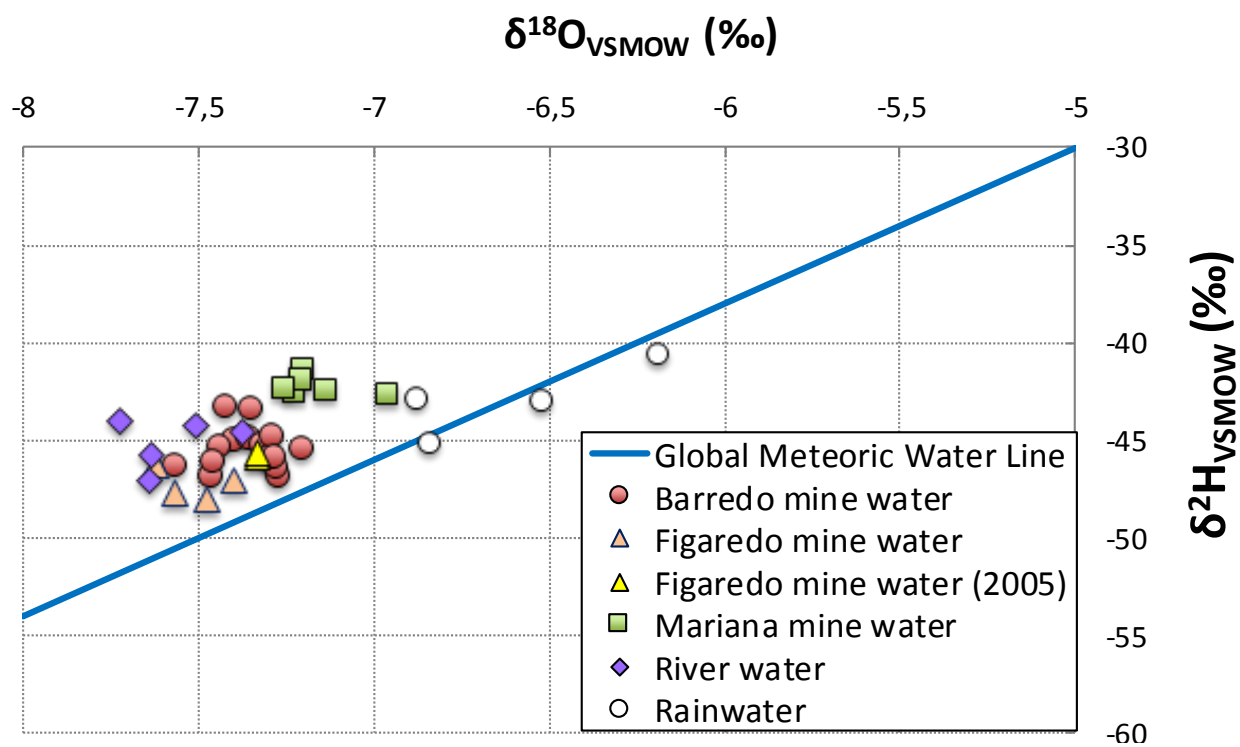


Fig. 4. a) Piper plot of Barredo and Figaredo waters sampled from 2005 to present; b) Time evolution of sulphate and Fe content in Barredo and Figaredo waters



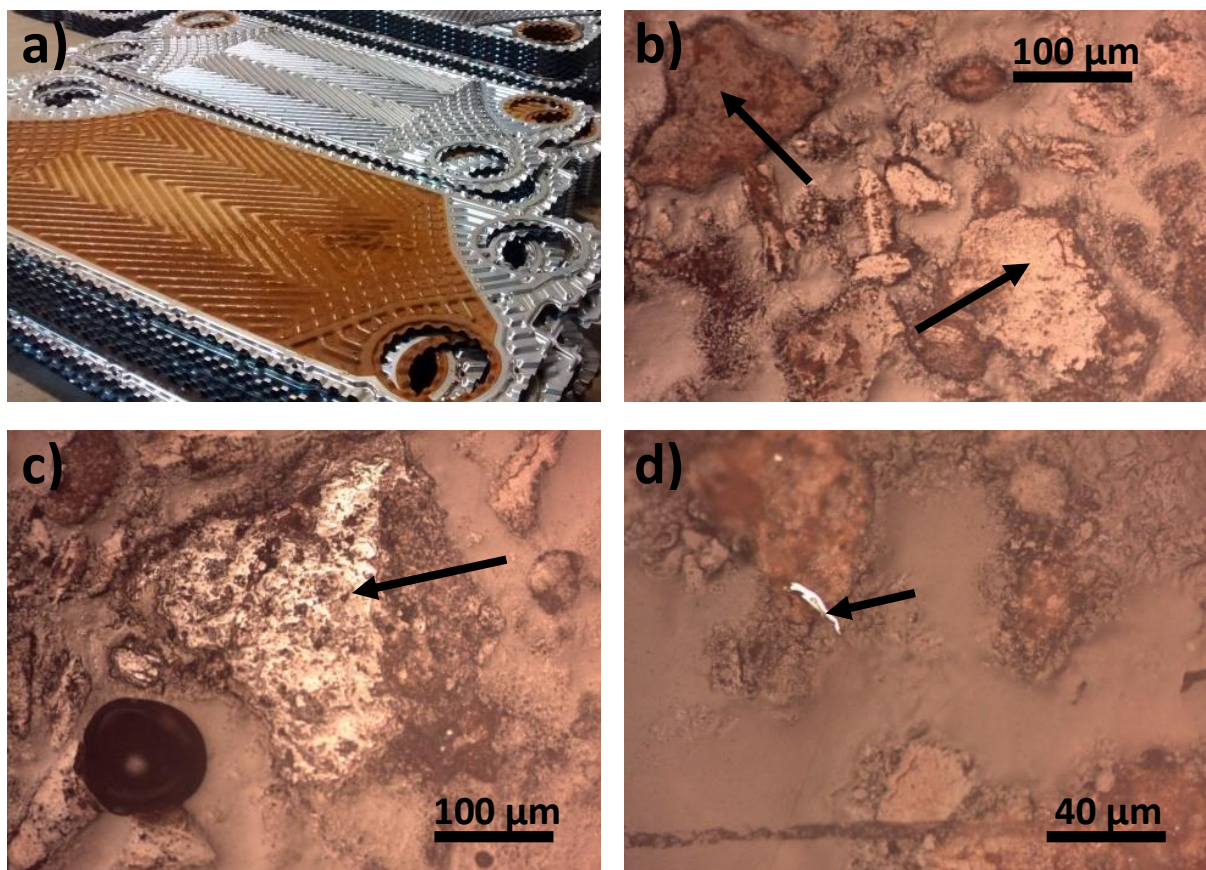


Fig. 6. a) Deposits clogging a heat exchanger plate; b) grey and brown grains of the Fe oxide that constitutes the principal component of these deposits; c) goethite grain with colloform internal texture; d) pyrite particle with marked reflectance. Images b, c and d taken with reflected light (parallel Nicols).